

A new multi-center approach to the exchange-correlation interactions in ab initio tight-binding methods

Pavel Jelínek^{1,2}, Hao Wang³, James P. Lewis³, Otto F. Sankey⁴ and José Ortega¹

¹ *Departamento de Física Teórica de la Materia Condensada,
Universidad Autónoma de Madrid, E-28049 Spain*

² *Institute of Physics, Academy of Sciences of the Czech Republic,
Cukrovarnická 10, 1862 53, Prague, Czech Republic*

³ *Department of Physics and Astronomy,
Brigham Young University, Provo, Utah 84602-4658, USA and*

⁴ *Department of Physics and Astronomy,
Arizona State University, Tempe, Arizona 85287-1504, USA*

(Dated: May 23, 2019)

Abstract

A new approximate method to calculate exchange-correlation contributions in the framework of first-principles tight-binding molecular dynamics methods has been developed. In the proposed scheme on-site (off-site) exchange-correlation matrix elements are expressed as a one-center (two-center) term plus a *correction* due to the rest of the atoms. The one-center (two-center) term is evaluated directly, while the *correction* is calculated using a variation of the Sankey-Niklewski [1] approach generalized for arbitrary atomic-like basis sets. The proposed scheme for exchange-correlation part permits the accurate and computationally efficient calculation of corresponding tight-binding matrices and atomic forces for complex systems. We calculate bulk properties of selected transition (W,Pd), noble (Au) or simple (Al) metals, a semiconductor (Si) and the transition metal oxide TiO_2 with the new method to demonstrate its flexibility and good accuracy.

I. INTRODUCTION

The application of first-principles simulation techniques is becoming a research tool of increasing importance in materials science, condensed matter physics and chemistry, and molecular physics and chemistry. Most of these techniques are based on Density Functional Theory (DFT) [2] which creates an important simplification of the many-body quantum mechanical problem. Typically, DFT calculations are performed within the Kohn-Sham approach [3] using the Local Density Approximation (LDA)[3] or a Generalized Gradient Approximation (GGA)[4]. These total energy quantum mechanical methods can be used to calculate forces on atoms, and thus perform first-principles molecular dynamics (MD) simulations. Such simulations have been very successful in the description of a variety of properties of different materials. But, in spite of the important simplifications introduced by DFT and related approximations (*e.g.* LDA,GGA), they still require a huge amount of computational resources. This problem has severely limited the range of applications of these simulation techniques to situations with small numbers of atoms (~ 100 -200) in the unit-cell, and short simulation times.

Due to the computational limitations, first-principles simulation techniques have been mainly directed to the study of the energetics and electronic structure of diverse materials, surfaces and molecules. Typically, a good guess for the atomic structure is obtained before the calculation, and the first-principles method is then used to refine the geometry, obtain the electronic structure, and to compare the total energy of a few competing structures. These methods, however, have been very rarely applied to elucidate complex atomic structures, that require the *exploration* of an extensive phase space of possibilities, when no *a priori* answer, or approximate good guess, is already available. More importantly, the application of first-principles methods to investigate complex kinetic processes in materials (*e.g.* the atomic motion of atoms on a surface, kinetic pathways, molecular reactions, etc) is still very limited, due to the computational resources required for these calculations.

It is clear that the usefulness of first-principles simulation techniques can be greatly extended if appropriate approximations are made, with the purpose of increasing the computational efficiency, with as little loss of accuracy as possible [5, 6, 7, 8, 9]. This idea has prompted the development of first-principles tight-binding molecular dynamics (TBMD) methods [1, 5, 6, 10], whose main characteristics are: (1) *a real-space* technique (*i.e.* no need

for super-cells or grids), (2) *optimized atomic-like orbitals* [1, 5, 11, 12] as basis set, and (3) efficient, two-dimensional, tabulation-interpolation schemes [1, 5] to obtain the effective TB Hamiltonian matrix elements as well as their derivatives to obtain the forces.

The main advantage of such techniques is computational efficiency which makes them ideal first-principles exploratory tools. The use of first-principles TBMD methods as a exploratory tool can be complemented with more accurate calculations, if necessary; once stimulating results or ideas are obtained, final results can be refined by performing more accurate and time-consuming calculations (plane-waves DFT - *e.g.*[13] - or even many-body - *e.g.* [14] - calculations).

In this paper we report on new developments for the treatment of exchange-correlation contributions in first-principles TBMD methods, and their implementation in the FIREBALL code [1, 15, 16]. The approximations used so far to handle these contributions are analyzed in Section II. In Section III we present our new approach to calculate the exchange-correlation contributions, and in Section IV we present some results for several materials to illustrate the performance of the new approach.

II. AB INITIO TIGHT BINDING: FIREBALL

FIREBALL [1, 15, 16] is a first-principles TBMD simulation technique based on a self-consistent version of the Harris-Foulkes [17, 18] functional. The energy functional is written as:

$$E_{TOT}[\rho(\vec{r})] = \sum_n \varepsilon_n - E_{ee}[\rho(\vec{r})] + E_{xc}[\rho(\vec{r})] - \int \rho(\vec{r}) V_{xc}[\rho(\vec{r})] d^3r + E_{ion-ion}, \quad (1)$$

where $\rho(\vec{r})$ is the *input density*, which will be allowed to vary, and will be determined selfconsistently. The first term is a sum over occupied eigenstates, ε_n , of the effective one-electron Hamiltonian,

$$\left(-\frac{1}{2}\nabla^2 + V[\rho] \right) \psi_n = \varepsilon_n \psi_n; \quad (2)$$

the potential V is the sum of the ionic potential, $v_{ion}(\vec{r})$, (typically represented by a pseudopotential), a Hartree potential, and an exchange-correlation potential V_{xc}

$$V[\rho] = v_{ion}(\vec{r}) + \int \frac{\rho(\vec{r}') d^3r'}{|\vec{r} - \vec{r}'|} + V_{xc}[\rho(\vec{r})]. \quad (3)$$

In equation (1) E_{ee} is an average electron-electron energy,

$$E_{ee}[\rho] = \frac{1}{2} \int \int \frac{\rho(\vec{r})\rho(\vec{r}')}{|\vec{r} - \vec{r}'|} d\vec{r}d\vec{r}', \quad (4)$$

$E_{ion-ion}$, is the ion-ion interaction energy

$$E_{ion-ion} = \frac{1}{2} \sum_{i,j} \frac{Z_i Z_j}{|\vec{R}_i - \vec{R}_j|} \quad (5)$$

(Z_i is the nuclear or pseudopotential charge of atom i at position \vec{R}_i), and $E_{xc}[\rho]$ is the exchange-correlation energy. First-principles MD simulations can be performed once the forces

$$\vec{F}_i = -\frac{\partial E_{TOT}}{\partial \vec{R}_i} \quad (6)$$

on each atom i are evaluated.

The efficiency of calculations based on the Harris functional is associated with the possibility to choose $\rho(\vec{r})$ in the above equations as a sum of atomic-like densities, $\rho_i(\vec{r})$:

$$\rho(\vec{r}) = \sum_i \rho_i(\vec{r}). \quad (7)$$

In the FIREBALL method, confined atomic-like orbitals are used as a basis set for the determination of the occupied eigenvalues and eigenvectors of the one-electron Hamiltonian, Eq. (2). The fireball orbitals, introduced by Sankey and Niklewski (SN) [1], are obtained by solving the atomic problem with the boundary condition that the atomic orbitals vanish outside and at a predetermined radius r_c where $\psi(\vec{r})|_{r=r_c} = 0$ (see Fig. 1). An important advantage of the fireball basis set is that the Hamiltonian (Eqn. (2)) and the overlap matrix elements are quite sparse for large systems. The electron density $\rho(\vec{r})$ is written in terms of the fireball orbitals $\phi_{ilm}(\vec{r}) \equiv \phi_\mu(\vec{r})$ (i is the atomic site, l represents the atomic subshell - *e.g.* $3s, 3p, 3d$, etc., and m is the magnetic quantum number)

$$\rho(\vec{r}) = \sum_\mu q_\mu |\phi_\mu(\vec{r})|^2. \quad (8)$$

In this way four-center integrals are not required for the calculation of the Hartree terms, and all the two- and three center interactions are tabulated beforehand and placed in interpolation data-tables which are no larger than two-dimensional [1]. Hamiltonian matrix elements are evaluated by looking up the necessary information from the data-tables.

In practice, the atomic densities ρ_i

$$\rho_i(\vec{r}) = \sum_{lm} q_{ilm} |\phi_{ilm}(\vec{r})|^2. \quad (9)$$

are approximated to be spherically symmetric around each atomic site i (*i.e.* $q_{ilm} = q_{ilm'}$). Self-consistency is achieved by imposing that the output orbital charges q_{μ}^{out} (obtained from the occupied eigenvectors ψ_n of equation (2)) and input orbital charges q_{μ} coincide (see ref. [15] and [19] for further details).

The remaining difficulty is the efficient calculation of exchange-correlation interactions within a first-principles TB scheme. One possibility is to use non-standard DFT and introduce the exchange-correlation energy and potential as a function of the orbital occupancies [9, 20, 21]. In this paper, however, we opt for the more traditional approach in which exchange-correlation contributions are calculated as a functional of the electron density $\rho(\vec{r})$. Within this line, two different methods have been previously proposed for the practical calculation of exchange-correlation terms, using data-tables similar to those for the Hartree contributions. These two methods are:

A. Sankey-Niklewski approximation

The basic idea introduced by SN [1] is to write down the non-linear in $\rho(\vec{r})$ exchange-correlation matrix elements in terms of matrix elements of $\rho(\vec{r})$. These later matrix elements are easily tabulated in data-tables no larger than two-dimensional, similar to those required for the Hartree terms.

Consider the matrix elements $\langle \phi_{\mu} | V_{xc}[\rho] | \phi_{\nu} \rangle$ of the exchange-correlation potential. For each matrix element $\langle \phi_{\mu} | V_{xc}[\rho] | \phi_{\nu} \rangle$, expand $V_{xc}[\rho]$ in a Taylor's series

$$V_{xc}[\rho] \simeq V_{xc}[\bar{\rho}_{\mu\nu}] + V'_{xc}[\bar{\rho}_{\mu\nu}](\rho - \bar{\rho}_{\mu\nu}) + \dots \quad (10)$$

around an appropriate “average density” $\bar{\rho}_{\mu\nu}$:

$$\bar{\rho}_{\mu\nu} = \frac{\langle \phi_{\mu} | \rho | \phi_{\nu} \rangle}{\langle \phi_{\mu} | \phi_{\nu} \rangle} \quad (11)$$

With this choice of $\bar{\rho}_{\mu\nu}$ the second term in the expansion for $\langle \phi_{\mu} | V_{xc}[\rho] | \phi_{\nu} \rangle$ is zero, and the next term is minimized [1]. This yields

$$\langle \phi_{\mu} | V_{xc}[\rho] | \phi_{\nu} \rangle \simeq \langle \mu | V_{xc}[\rho] | \nu \rangle \simeq V_{xc}[\bar{\rho}_{\mu\nu}] \langle \mu | \nu \rangle \quad (12)$$

SN [1] realized that corrections to this approximation are required for the case $\langle \phi_\mu | \phi_\nu \rangle \equiv \langle \mu | \nu \rangle = 0$, and they devised a scheme to add those corrections specifically for a minimal sp^3 basis set.

The first step towards improved exchange-correlation contributions in our TBMD scheme (see Sec. III) will be, precisely, to extend their ideas for a general atomic-like basis set. Also, it will be shown below that the SN average density approximation is not accurate for the exchange-correlation-energy on-site terms $\langle \mu | \epsilon_{xc} | \mu \rangle$ for atoms with a significant valence electron density such as transition metals (e.g. Au, Ag, Pd, etc.); in Sec. III we will present a new scheme that corrects this problem.

B. Horsfield approximation

An alternative approach to deal with exchange-correlation terms within a first-principles TBMD method was proposed by Horsfield [5], who introduced a many-center expansion based on Eqn. (7). In this approach we can distinguish two cases [5] (i_μ is the atomic site corresponding to orbital μ and i_ν corresponds to orbital ν),

(a) $i_\mu = i_\nu \equiv i$

$$\langle \mu | V_{xc}[\rho] | \nu \rangle \simeq \langle \mu | V_{xc}[\rho_i] | \nu \rangle + \sum_{j \neq i} \langle \mu | (V_{xc}[\rho_i + \rho_j] - V_{xc}[\rho_i]) | \nu \rangle, \quad (13)$$

(b) $(i_\mu \equiv i) \neq (i_\nu \equiv j)$

$$\langle \mu | V_{xc}[\rho] | \nu \rangle = \langle \mu | V_{xc}[\rho_i + \rho_j] | \nu \rangle + \sum_{k \neq i, j} \langle \mu | (V_{xc}[\rho_i + \rho_j + \rho_k] - V_{xc}[\rho_i + \rho_j]) | \nu \rangle. \quad (14)$$

Although practical experience has shown that this is an accurate approach in many cases, the on-site terms (case (a)) are not always well-approximated by the above equation, and additional numerical integrals are necessary for those term [5, 6]. Another shortcoming of this approach is the fact that most of the computational time required to create the data-tables within this approximation is spent in the calculation of the exchange-correlation terms, reducing the computational efficiency.

III. A NEW EXCHANGE-CORRELATION SCHEME FOR AB INITIO TIGHT-BINDING

We now present a new approximation to calculate exchange-correlation contributions in a first-principles TBMD method. This new approximation is composed of two main parts. First, we generalize the SN approximation for an arbitrary atomic-like basis set. Second, we propose an improved approximation which combines the best features of both the SN and Horsfield approximations.

To generalize the SN approach beyond sp^3 basis sets, we define average densities $\bar{\rho}_{\mu\nu}$ using auxiliary, spherically symmetric orbitals φ_{il} (defined below). The use of these spherically symmetric orbitals solves problems associated with the zero overlap $\langle \mu | \nu \rangle = 0$ cases; moreover, this approach for calculating exchange-correlation terms is consistent with the spherical approximation used in calculating Hartree terms.

We define spherically symmetric orbitals $\varphi_{il} \equiv \varphi_{\mu}$ for each atomic subshell (i, l) , corresponding to atomic-like orbitals ϕ_{ilm} as follows. First, we consider the atomic-like orbitals

$$\phi_{ilm} = \omega_{il}(r)Y_{lm}(\Omega) \quad (15)$$

where $\omega_{il}(r)$ is the radial part of ϕ_{ilm} and $Y_{lm}(\Omega)$ the spherical harmonic associated with the angular part. Next, we define the spherically symmetric orbitals by

$$\varphi_{il} = \tilde{\omega}_{il}(r)Y_{00}(\Omega) \quad (16)$$

where $\tilde{\omega}$ is the positive root of $(\omega)^2$ (see Fig. 1); $\tilde{\omega}$ is defined this way in order to avoid spurious cancellations in the importance sampling calculation of $\bar{\rho}_{\mu\nu}$ (Eq. 17) which occur with certain intra-atomic cases (e.g. two different s-orbitals on the same atom).

With these auxiliary orbitals we now define average densities for each matrix element (μ, ν) as

$$\bar{\rho}_{\mu\nu} = \frac{\langle \varphi_{\mu} | \rho | \varphi_{\nu} \rangle}{\langle \varphi_{\mu} | \varphi_{\nu} \rangle} \quad (17)$$

This new definition for the average densities $\bar{\rho}_{\mu\nu}$ (using the auxiliary orbitals φ instead of the atomic orbitals ϕ) solves all problems related to zero overlap ($\langle \phi_{\mu} | \phi_{\nu} \rangle = 0$), since now $\langle \varphi_{\mu} | \varphi_{\nu} \rangle \neq 0$; moreover, the use of auxiliary orbitals represents an improvement in the ‘‘importance sampling’’ calculation of $\bar{\rho}_{\mu\nu}$ for the non-zero overlap cases. Regions of positive

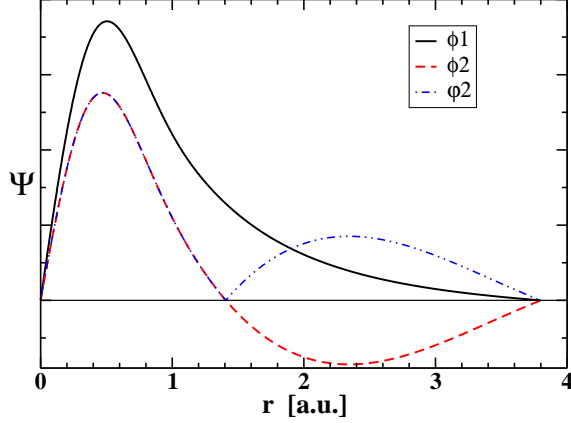


FIG. 1: Two radial functions corresponding to Fireball ϕ_1 and ϕ_2 , and auxiliary φ_2 orbital. The auxiliary orbital φ_1 (not shown) coincides with ϕ_1 .

overlap are no longer “artificially” canceled by regions of negative overlap: both positive and negative overlap regions add-up now in this new definition of $\bar{\rho}_{\mu\nu}$.

Note that since the orbitals φ_{il} are spherically symmetric, the same value of $\bar{\rho}_{\mu\nu}$ is obtained for all the matrix elements (μ, ν) associated with a given pair of atomic subshells $(i, l; i', l')$. Also with our new definition of $\bar{\rho}_{\mu\nu}$, we have in general $\langle \mu | \rho | \nu \rangle \neq \bar{\rho}_{\mu\nu} \langle \mu | \nu \rangle$, and we keep the next term in the Taylor’s expansion for $V_{xc}[\rho]$:

$$\langle \mu | V_{xc}[\rho] | \nu \rangle \simeq V_{xc}[\bar{\rho}_{\mu\nu}] \langle \mu | \nu \rangle + V'_{xc}[\bar{\rho}_{\mu\nu}] \left(\langle \mu | \rho | \nu \rangle - \bar{\rho}_{\mu\nu} \langle \mu | \nu \rangle \right) \quad (18)$$

We refer to this approximation as the generalized SN approach (GSN approach).

The average density approximation is not very accurate for certain matrix elements, particularly $\langle \mu | \epsilon_{xc} | \mu \rangle$. This is not a serious problem (as we demonstrate in Sec. IV) for the determination of the structural and/or electronic properties, since basically only the absolute value of the total energy is affected (*i.e.* it represents a rigid shift in the total energy). Nevertheless, the next step in our new approximation is to correct this inaccuracy. For this purpose, we use the best features of the SN and the Horsfield approximations. As in the Horsfield scheme, we distinguish two cases: (a) on-site ($i_\mu = i_\nu$), and (b) off-site matrix elements.

(a) $i_\mu = i_\nu \equiv i$. As a first step in our approximation, we simply add and subtract a contribution associated with the atomic density ρ_i at site i , and write, *formally*, the

matrix element as a one-center contribution plus a *correction*, in similarity with the Horsfield approach:

$$\langle \mu | V_{xc}[\rho] | \nu \rangle = \langle \mu | V_{xc}[\rho_i] | \nu \rangle + \left(\langle \mu | V_{xc}[\rho] | \nu \rangle - \langle \mu | V_{xc}[\rho_i] | \nu \rangle \right). \quad (19)$$

The one-center (first) term is easily calculated and tabulated, and we use the GSN approach discussed above to evaluate the *correction*:

$$\begin{aligned} \langle \mu | V_{xc}[\rho] | \nu \rangle &\simeq \langle \mu | V_{xc}[\rho_i] | \nu \rangle \\ &+ V_{xc}[\bar{\rho}_{\mu\nu}] \langle \mu | \nu \rangle + V'_{xc}[\bar{\rho}_{\mu\nu}] \left(\langle \mu | \rho | \nu \rangle - \bar{\rho}_{\mu\nu} \langle \mu | \nu \rangle \right) \\ &- V_{xc}[\bar{\rho}_i] \langle \mu | \nu \rangle - V'_{xc}[\bar{\rho}_i] \left(\langle \mu | \rho_i | \nu \rangle - \bar{\rho}_i \langle \mu | \nu \rangle \right) \end{aligned} \quad (20)$$

with

$$\bar{\rho}_i = \frac{\langle \varphi_\mu | \rho_i | \varphi_\nu \rangle}{\langle \varphi_\mu | \varphi_\nu \rangle} \quad (21)$$

(indices μ, ν have been omitted in $\bar{\rho}_i$, for clarity).

(b) ($i_\mu = i$) \neq ($i_\nu = j$). Proceeding in a similar manner as for the on-site matrix elements, we obtain for the off-site matrix elements:

$$\begin{aligned} \langle \mu | V_{xc}[\rho] | \nu \rangle &= \langle \mu | V_{xc}[\rho_i + \rho_j] | \nu \rangle + \left(\langle \mu | V_{xc}[\rho] | \nu \rangle - \langle \mu | V_{xc}[\rho_i + \rho_j] | \nu \rangle \right) \quad (22) \\ &\simeq \langle \mu | V_{xc}[\rho_i + \rho_j] | \nu \rangle \\ &+ V_{xc}[\bar{\rho}_{\mu\nu}] \langle \mu | \nu \rangle + V'_{xc}[\bar{\rho}_{\mu\nu}] \left(\langle \mu | \rho | \nu \rangle - \bar{\rho}_{\mu\nu} \langle \mu | \nu \rangle \right) \\ &- V_{xc}[\bar{\rho}_{ij}] \langle \mu | \nu \rangle - V'_{xc}[\bar{\rho}_{ij}] \left(\langle \mu | (\rho_i + \rho_j) | \nu \rangle - \bar{\rho}_{ij} \langle \mu | \nu \rangle \right) \end{aligned} \quad (23)$$

with

$$\bar{\rho}_{ij} = \frac{\langle \varphi_\mu | (\rho_i + \rho_j) | \varphi_\nu \rangle}{\langle \varphi_\mu | \varphi_\nu \rangle} \quad (24)$$

(indices μ, ν omitted for clarity). In Eqs. (20) and (23) $\bar{\rho}_{\mu\nu}$, which includes all density contributions, is defined using Eq. (17).

IV. RESULTS

In this section we present results illustrating the performance of our new exchange-correlation scheme discussed in section III. Transition metals contain a significant valence electron density (the *d*-electrons), mixed with a free-electron-like density (the *sp*-bands),

and thus represent good test cases for the different exchange-correlation schemes. In this section we present results for some transition metals (Au, Pd, W), and the transition metal oxide TiO_2 ; we also show some results for a typical sp^3 metal (Al) and a semiconductor (Si).

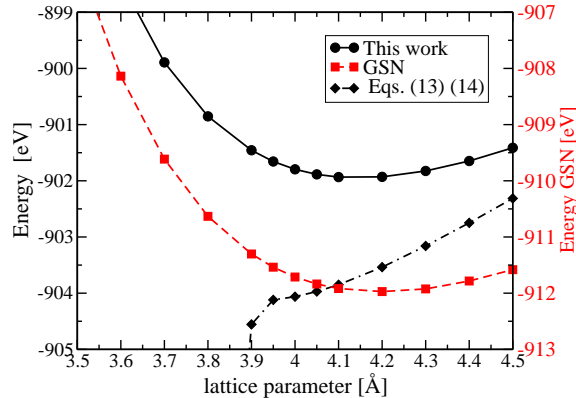


FIG. 2: Total energy for bulk Au as a function of the lattice parameter a for different XC-approximations presented in this work. The energy scale on the right corresponds to the GSN approximation. 'This work' line shows the result obtained from Eqs. 20 and 23. The dashed line is the result obtained using Eqs. 13 and 14. Basis set: sp^3d^5 fireball orbitals with cut-off radii $R_c(s) = 4.6$ a.u., $R_c(p) = 5.2$ a.u. and $R_c(d) = 4.1$ a.u.

As an example we plot energy vs. lattice constant for Au. Fig. 2 shows the total energy of bulk Au as a function of the lattice parameter as calculated with the FIREBALL code using the new exchange-correlation scheme proposed in section III (*i.e.* Eqs. (20) and (23)). We used a sp^3d^5 basis set with fireball orbitals defined by the following cut-off radii: $R_c(s) = 4.6$ a.u., $R_c(p) = 5.2$ a.u. and $R_c(d) = 4.1$ a.u. Also we show in the results for GSN (equation (18)), and Horsfield (obtained using Eqs. (13) and (14), *i.e.* without the additional numerical integral for the on-site terms). These results demonstrate how critical it is for the transition metals to have a good description of the on-site XC-contributions. Note the nearly rigid shift of the GSN result (scale on the right of Fig. 2) by ~ 10 eV. As mentioned in Secs. II and III, this is related to the inaccuracy of the average-density approximation (Eq. 18) for calculating the on-site energy terms $\langle \mu | \epsilon_{xc} | \mu \rangle$: Au atoms contain a large electron density (~ 10 d -electrons plus 1 s -electron) in the valence band. For comparison, this shift is only ~ 0.7 eV in the case of bulk Al.

TABLE I: Equilibrium lattice constants a and bulk moduli B for selected elements obtained using Eqs. 20 and 23 (This work), and Eq. 18 (GSN) for the exchange-correlation LDA contributions. We calculated these with sp^3 (Al,Si) or sp^3d^5 (transition metals) basis sets of fireball orbitals with cut-off radii R_c (in a.u.) as indicated. Also shown are PW-LDA and experimental values.

Name	Structure	Basis set	a (Å)				B (GPa)			
			This work	GSN	PW-LDA	Expt.	This work	GSN	PW-LDA	Expt.
Au	fcc	s4.6-p5.2-d4.1	4.14	4.21	4.06	4.07	210	197	205	171
Pd	fcc	s4.6-p5.0-d4.0	3.96	3.98	3.85	3.89	215	294	220	181
W	bcc	s4.7-p5.2-d4.5	3.18	3.17	3.14	3.17	347	320	333	310
Si	zbd	s4.8-p5.4	5.46	5.50	5.38	5.43	109	98	96	100
Al	fcc	s5.3-p5.7	4.04	4.09	3.97	4.05	93	85	84	76

Table I shows the calculated lattice parameter a and Bulk modulus B_0 (obtained using a Murnaghan equation of state EOS) for Au, as well as for other transition metals (Pd, W), Al (a typical free-electron-like metal) and for Si (a typical semiconductor). These results have been obtained using either minimal sp^3 basis sets (Al,Si) or sp^3d^5 basis sets (transition metals). The experimental values [22], and the plane-waves LDA values (PW-LDA), are also presented in Table I. This Table shows that with the new approach to introduce exchange-correlation contributions the experimental lattice constants a are reproduced within $\sim 2\%$ while the bulk moduli are slightly overestimated by $\sim 15\%$. The agreement is improved when comparing with the PW-LDA. Since the accuracy of first-principles TBMD methods is mainly related with the quality of the atomic-like basis set, improvements on the results presented in Table I are to be expected with a better choice for the basis set, either by improving the sp^3 or sp^3d^5 orbitals *and/or* adding new orbitals to the basis set (*e.g.* double basis sets, etc.) [12, 23, 24, 25].

Figures 3,4,5 show the band-structures for the transition metals Au, W and Pd. The comparison with more accurate calculations (*e.g.* see [26]) shows that the band-structures are well-approximated within the present first-principles TB-scheme. In this case, there is practically no difference between the band-structures obtained with the GSN or the new approach (equations (20,23)).

Tetragonal rutile structure TiO_2 belongs to the space group $P4_1/mnm$, containing 6

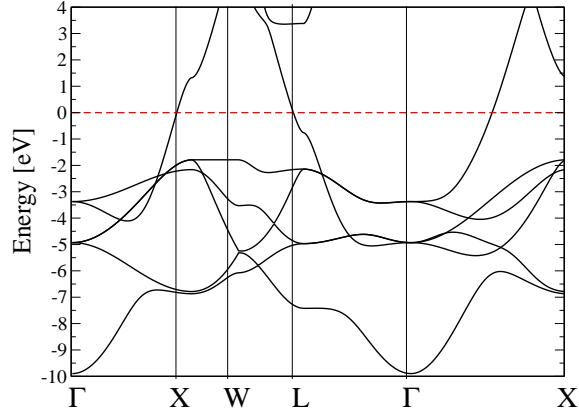


FIG. 3: Band structure of Au fcc. LDA exchange-correlation terms are calculated using the new approximation discussed in Sec. III. Basis set: sp^3d^5 fireball orbitals with cut-off radii $R_c(s) = 4.6$ a.u., $R_c(p) = 5.2$ a.u. and $R_c(d) = 4.1$ a.u.. The dashed line represents the Fermi level.

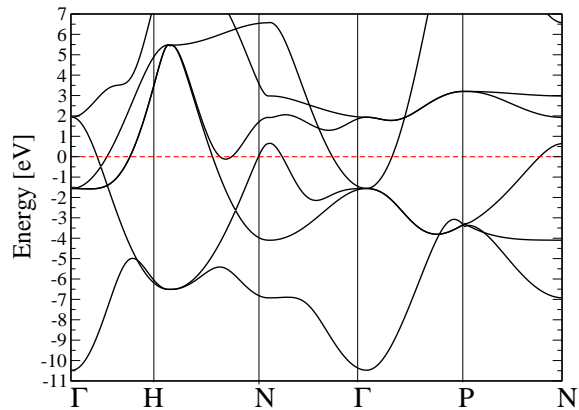


FIG. 4: Band structure of W bcc (see also Fig. 3). Basis set: sp^3d^5 fireball orbitals with cut-off radii $R_c(s) = 4.7$ a.u., $R_c(p) = 5.2$ a.u. and $R_c(d) = 4.5$ a.u..

atoms per unit cell. The structural parameters for rutile structure TiO_2 have been determined to a high degree of accuracy from the neutron diffraction experiments performed by Burdett *et al.* [27]. We have calculated the structural parameters and electronic bandstructure for TiO_2 in the rutile structure using the FIREBALL code and the exchange-correlation approach discussed in section III. For these calculations we have used a sp^3 basis for oxygen with cut-off radii $R_c(s) = 3.6$ a.u. and $R_c(p) = 4.1$ a.u., while for Ti a basis set of sp^3d^5 orbitals was used, with cut-off radii $R_c(s) = 6.3$ a.u., $R_c(p) = 6.0$ a.u. and $R_c(d) = 5.7$ a.u. The optimal structure is obtained by minimizing the total energy of the rutile ($P4_1/mnm$) structures with respect to the lattice parameters a , c , and internal parameter u . We perform

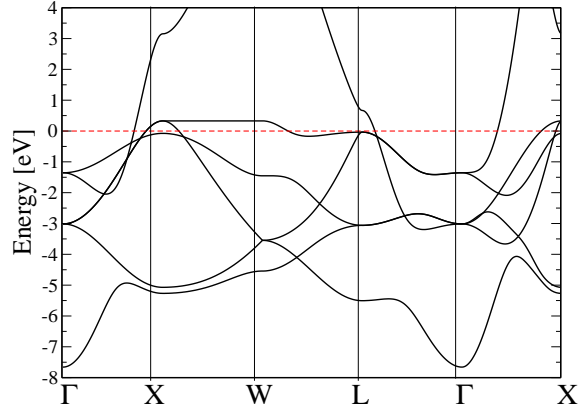


FIG. 5: Band structure of Pd fcc (see also Fig. 3). Basis set: sp^3d^5 fireball orbitals with cut-off radii $R_c(s) = 4.6$ a.u., $R_c(p) = 5.0$ a.u. and $R_c(d) = 4.0$ a.u..

this minimization by a two-step procedure as outlined in Ref.[28]. Table II summarizes the comparison of our results to the experimentally determined structural and elastic parameters in TiO_2 ; results from other theoretical works are also listed. This table shows that our results for the structural properties of TiO_2 in the rutile structure are within 1% of the experimental results of Burdett, *et al.* [27]. From the integrated EOS, we obtain a value for the bulk modulus B of 206 GPa which agrees well with the experimental value of 211 GPa [29]. In addition, our results agree well with the calculated results of others [28, 30].

TABLE II: Theoretical results for structural and elastic parameters for TiO_2 in the rutile structure. Comparisons are made between our results and experimental results for the volume V , lattice parameters a , c , internal parameter u , and bulk modulus B ; zero subscript represents the experimental results [27].

	V/V_0	a/a_0	c/c_0	u/u_0	B (GPa)	B_0 [29] (GPa)
Present work	0.994	0.997	0.999	0.994	206	211
Other calculation [28]	1.039	1.013	1.002	1.001	240	
Other calculation [30]	1.021	0.999	1.002	0.998	209	

Using our theoretically predicted equilibrium lattice parameters, we have calculated the self-consistent electronic band structure for rutile TiO_2 depicted in Fig. 6 along the high-symmetry directions of the irreducible Brillouin zone. Table III gives a summary of our

results in comparison to experiment and other calculations for the detailed features of the band structure. The upper valence band is composed of O_{2p} orbitals and has a width of 5.75 eV. These results are in agreement with the experimental values of 5.50 eV [31]. The lower O_{2s} band is 1.89 eV wide. Our results are consistent with other calculations [28, 30]. The calculated direct band gap at Γ of 3.05 eV is in agreement with the reported experimental gap of 3.06 eV [32]. The LDA generally underestimates the experimental band gap for insulators and semiconductors, and the band gap obtained from *ab initio* plane-wave calculations for TiO_2 is ~ 2.0 eV [28]. This underestimating effect of LDA is compensated in our results because we use a local orbital basis set. We also find an indirect band gap from Γ to M which is smaller than the direct band gap by 0.13 eV.

TABLE III: Comparison of our present work to the experimentally determined electronic properties for TiO_2 in the rutile structure. Definition of listed quantities are as follows: (1) $E_g - D$ is the direct bandgap (Γ to Γ), (2) $E_g - ID$ is the indirect bandgap (Γ to M), (3) E_{VB} is the upper valence bandwidth, and (4) $E_{O_{2s}}$ is the Oxygen 2s state bandwidth.

Structure	$E_g - D$ (eV)	E (eV) $_g - ID$	E_{VB} (eV)	$E_{O_{2s}}$ (eV)
Present	3.05	2.92	5.75	1.89
Experiments	3.06 [32]		5.50 [31]	
Others	1.78 [30], 2.00 [28]	3.00 [30], 2.00 [28]	6.22 [30], 5.7 [28]	1.94 [30], 1.80 [28]

V. SUMMARY

In summary, we have presented a new approach to calculate exchange-correlation contributions in first-principles TBMD methods. After a brief presentation of the basic theoretical foundations and practical motivation for these techniques, we have discussed the different approximations (SN [1] and Horsfield [5]) used so far to calculate exchange-correlation terms in these methods, using standard DFT (*e.g.* LDA). Then, in section III, we propose a new approach that corrects the main deficiencies of previous approximations in a practical manner (keeping always in mind computational efficiency). In this approach, on-site (off-site) exchange-correlation matrix elements are formally written as a one-center (two-center)

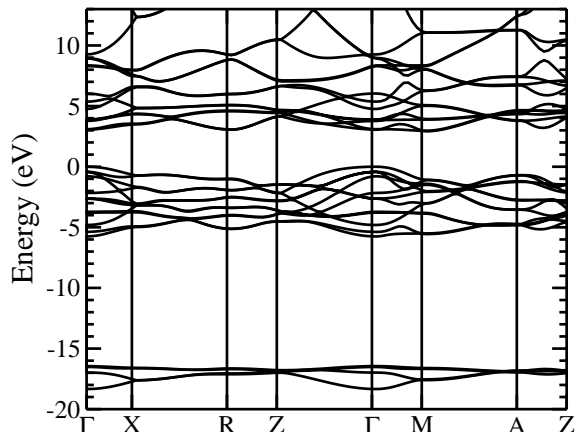


FIG. 6: Band structures for TiO_2 in the rutile structure. The valence-band maximum is taken as the zero of energy.

term plus a *correction* due to the rest of the atoms. The one-center (two-center) term is evaluated (and tabulated) directly, while the *correction* is calculated using the SN approach. For this purpose, a general (*i.e.* for arbitrary atomic-like basis set) version of the GSN approach has been also developed.

The new scheme has been tested for some materials using the FIREBALL code and minimal sp^3 (for Al, Si and O) or sp^3d^5 (Au, Pd, W, Ti) basis sets. The results, presented in section IV, show the good accuracy of the present first-principles TBMD approach as compared with experiment and other accurate calculations.

Acknowledgments

P.J. gratefully acknowledges financial support by the Spanish Ministerio de Educacion, Cultura y Deportes. This work has been supported by the DGI-MCyT (Spain) under contracts MAT2001-0665 and MAT2001-01534. J.P.L. and H.W. greatly acknowledges financial support from DOE Grant No. DE-FG02-03ER46059 and from the Center for the Simulation of Accidental Fires and Explosions (C-SAFE at the University of Utah), funded by the Department of Energy, Lawrence Livermore National Laboratory, under subcontract

-
- [1] O. F. Sankey and D. J. Niklewski, Phys. Rev. B **40**, 3979 (1989).
- [2] P. Hohenberg and W. Kohn, Phys. Rev. **136**, B864 (1964).
- [3] W. Kohn and L. J. Sham, Phys. Rev. **140**, A1133 (1965).
- [4] A.D.Becke, Phys. Rev. A **38**, 3098 (1988).
- [5] A.P. Horsfield, Phys. Rev. B **56**, 6594 (1997).
- [6] A.P. Horsfield and A.M. Bratkovsky, J. Phys.: Condens. Matter **12** R1 (2000).
- [7] D. Porezag et al., Phys. Rev. B **51**, 12947 (1995); T. Freuenheim et al. Phys. Rev. B **52**, 11492 (1995).
- [8] P. Ordejon, E. Artacho, J.M. Soler, Phys. Rev. B **53**, 10441 (1996); D. Sanchez-Portal, P. Ordejon, E. Artacho and J.M. Soler, Int. J. Quant. Chem. **65**, 453 (1997).
- [9] P. Pou et al., Int. J. Quant. Chem. **91**, 151 (2003); R. Oszwaldowski et al., J. Phys.: Cond. Matter **15**, S2665 (2003).
- [10] J. Ortega, Computational Materials Science **12**, 192 (1998).
- [11] H. Eschrig and I. Bergert, Phys. Stat. Sol. B **90**, 621 (1978).
- [12] J. Junquera, O. Paz, D. Sánchez-Portal and E. Artacho, Phys. Rev. B **64**, 235111 (2001).
- [13] J. Ortega, R. Pérez and F. Flores and A. Levy Yeyati, J. Phys.: Condens. Matter **12**, L21 (2000).
- [14] J. Ortega, F. Flores and A. Levy Yeyati, Phys. Rev. B **58**, 4584 (1998).
- [15] A.A. Demkov, J. Ortega, O.F. Sankey and M.P. Grumbach, Phys. Rev. B **52**, 1618 (1995).
- [16] J.P. Lewis *et al.*, Phys. Rev. B **64**, 195103 (2001).
- [17] J. Harris, Phys. Rev. B **31**, 1770 (1985).
- [18] W. Foulkes and R. Haydock, Phys. Rev. B **39**, 12520 (1989).
- [19] J.P. Lewis, J. Pikus, Th. E. Cheatham, E.B. Starikov, H. Wang, J. Tomfohr, and O.F. Sankey, Phys. Stat. Sol. **233**, 90 (2002).
- [20] F.J. Garcia-Vidal et al., Phys. Rev. B **50**, 10537 (1994).
- [21] P.Pou et al. Phys. Rev. B **62**, 4309 (2000).
- [22] C. Kittel, Introduction to Solid State Physics, 6th ed. (Wiley, New York, 1986).
- [23] S.D. Kenny, A.P. Horsfield and Hideaki Fujitani, Phys. Rev. B **62**, 4899 (2000).

- [24] E. Anglada, J.M. Soler, J. Junquera and E. Artacho, Phys. Rev. B **66**, 205101 (2002).
- [25] T. Ozaki and H. Kino, Phys. Rev. B **69**, 195113 (2004).
- [26] D.A. Papaconstantopoulos, Handbook of the Band Structure of Elemental Solids, (Plenum Press, New York, 1986).
- [27] J. K. Burdett, T. Hughbanks, G. J. Miller, J. W. Richardson, and J. V. Smith, I. Am. Chem. Soc. **109**, 3639(1987).
- [28] K. M. Glassford and J. R Chelikowsky, Phys. Rev. B **46**, 1284 (1992).
- [29] T. Arlt, M. Bermejo, M. A. Blanco, L. Gerward, J. Z. Jiang, J. S. Olsen, and J. M. Recio, Phys. Rev. B **61**, 14414 (2000).
- [30] S. D. Mo amd W. Y. Ching, Phys. Rev. B **51**, 13023 (1995).
- [31] S. P. Kowalczyk, F. R. McFeely, L Ley, V. T. Gritsyna, and D. A. Shirley, Solid State Commun. **23**, 161 (1977).
- [32] J. Pascual and H. Mathieu, Phys. Rev. B **18**, 5606 (1978).
- [33] K. Vos, J. Phys. C: Solid State Phys. **10**, 3917 (1977).
- [34] R. V. Kasowski and R. H. Tait, Phys. Rev. B **20**, 5168 (1979).